

MACROSCOPIC INSPECTION

Following photo-documentation, all tiles were systematically scanned with the naked eye, aided by a hand lens and a flexible, fiber-optic light source to provide variable geometries of illumination. We found that a combination of back and side lighting is best for optimum viewing of impact features of various sizes and geometry in aerogel. This first-order inspection aimed at identifying and cataloging the occurrence of all features > 2 mm in diameter or length, including their relative frequency. Each feature was classified and recorded on a transparent overlay of the

individual mug shots. Even the most cursory inspection reveals morphologically distinct classes of impact features, including transitional stages among some. Three basic types of features were distinguished during this macroscopic inspection: (a) *tracks*, (b) *pits* and (c) very *shallow depressions*. Figure 15 contrasts a classical, slender penetration track with a substantially hemispherical pit to simply illuminate the existence of dramatically different features and the need for their classification. We will augment the macroscopic observations of these features with detailed microscopic observations below, to provide a more complete and detailed morphologic description. Such microscopic investigations not only corroborate the macroscopic appearance and classification scheme, but they validated and extended this scheme to very small sizes beyond the resolution of the unaided eye. In addition, the microscopic investigation revealed the existence of specific subclasses of features and the transitional nature of some.

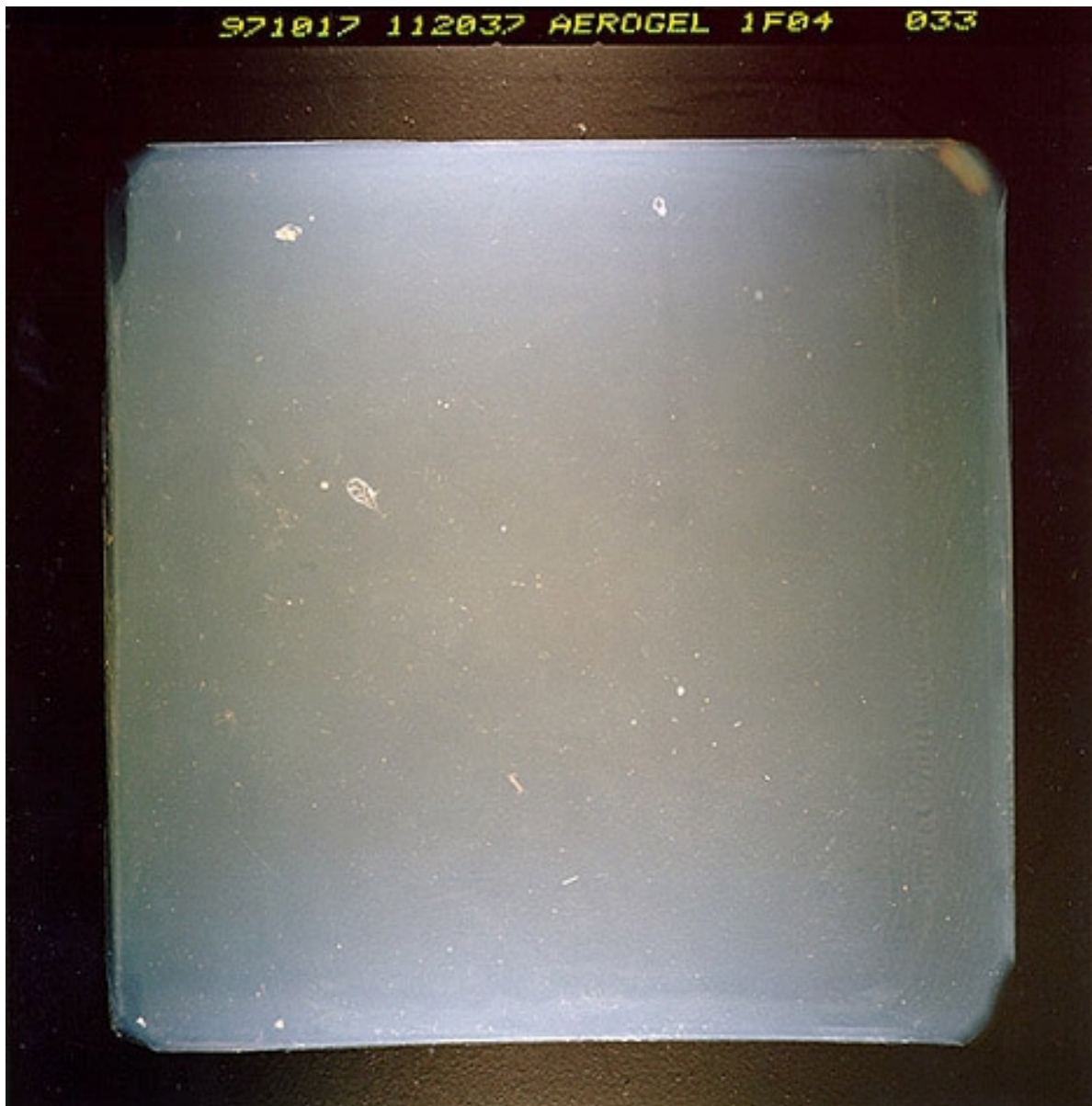


Figure 14. ODC collector mug shot showing tile 1F04 that exhibits a more typical track density.

The major criterion employed in classifying the various features was their aspect ratio, defined as the absolute length or depth (L) relative to its diameter (D). The D/L values vary widely from 0.1 to 40. In contrast, most hypervelocity craters in space-exposed metal surfaces have relatively constant diameter/depth relationships, clustering prominently around 0.5 to 0.6 (e.g., Humes, 1991 or Love *et al.*, 1995). The wide range of D/L values in aerogel attests to the superior sensitivity of a very low-density target in recording and preserving highly variable initial impact conditions (e.g., projectile density, shape, and/or impact velocity). It also introduces complexity into the description and interpretation of aerogel features, as total track length is the most

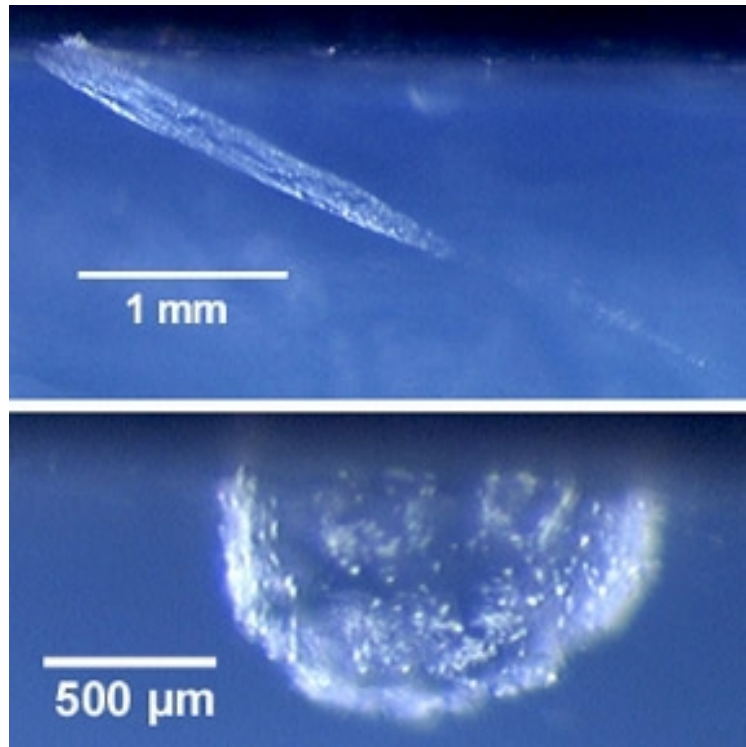


Figure 15. Examples of a typical *track* and *pit*, illustrating their dramatically different morphologies and the need for detailed morphological classification of all impact features in low-density aerogel.

significant parameter for very slender tracks. However, we sense that the feature diameter becomes increasingly more important in the understanding of progressively shallower and ultimately hemispherical pit structures.

We define D as the largest diameter of a feature, typically encountered at some depth below the aerogel surface. This maximum diameter is generally larger, commonly by factors of 2 - 4, than the actual projectile entrance hole at the aerogel surface. We classified features as *tracks* if they possessed an $L/D > 10$, or as *pits* if $0.5 > L/D < 10$, and as *shallow depressions* for L/D of < 0.5 . However, the L/D ratio is merely an important guide towards the classification of all impact features and (rare) exceptions to the above rules are permitted; L/D changes continuously and there are transitional cases. Additional classification criteria may be used, such as the presence or absence of melt-phenomena, pervasively crushed zones of aerogel, or the absence or presence of copious amounts of particulate residue.

Tracks

Tracks are defined as the classic, carrot-shaped, relatively straight and deep penetrations known from any number of experimental impact studies into highly porous and low-density media as summarized by Tsou (1990; 1995), or Hörz *et al.* (1997). The L/D values for ODC tracks are by definition > 10 , yet they are commonly on the order of 20 - 30. A typical ODC track and an example of an experimental track are illustrated in Figure 16, including enlargements of the major morphologic components. Most tracks have entrance holes at the surface of the aerogel collector that are smaller than the diameters of subsequent track sections

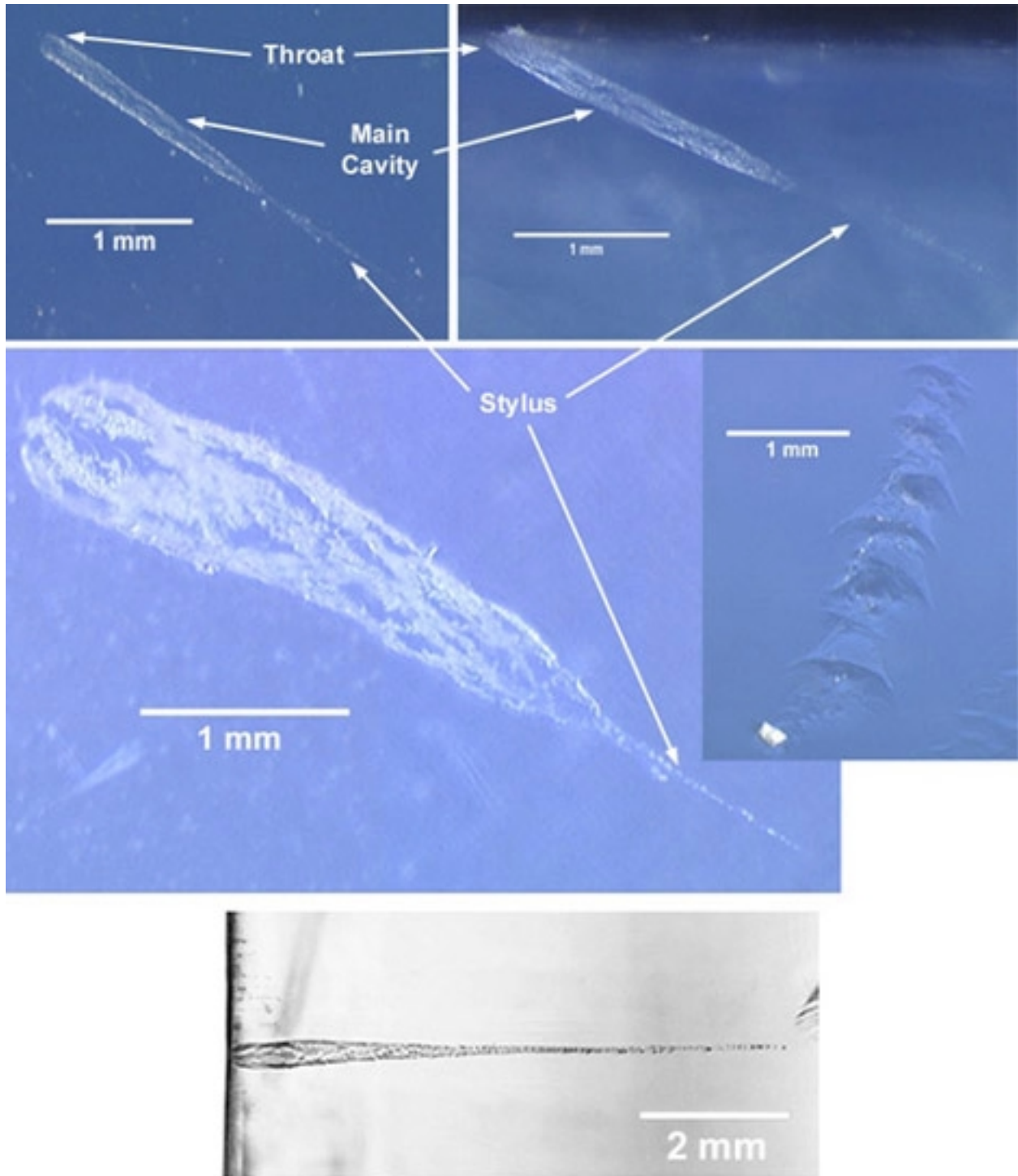


Figure 16. Morphological elements and definition of terms for an ODC track, and comparison with an experimental analog produced by a 50 μm diameter glass sphere at 6 km/s.

(Burchell and Thomson, 1996). Such tracks tend to begin to substantially widen immediately after penetration of the aerogel surface, resulting in a relatively large diameter and rather long cavity, which may be as long as some 30 to 50% of the total track length. The wide diameter and length of this cavity account for most of the aerogel mass that was displaced or deformed, and is

the reason we refer to this portion of a track as its *main cavity*. For descriptive ease, we refer to the near surface portions of such cavities as the track's *throat*, which terminates when the maximum diameter (D) of the track is reached. By definition, the remainder of the main cavity decreases continuously with depth, yet at highly variable rates. Very long, slender cones may contrast with cavities that are substantially cylindrical in shape or that are distinctly bulbous, while rare specimen decrease their diameters in a distinctly stepwise fashion. The detailed geometry of the main cavities of such features can vary considerably, yet they all taper into a long and slender, needle-like structure at depth, which we refer to as the track's *stylus*. This stylus can also occupy a substantial fraction of the total penetration path, commonly as much as 50% or more. It is the presence or absence of this slender, needle-like stylus that places such a feature as a genuine track.

In contrast to the main cavity, the stylus continuously tapers to the final tip, which we refer to as the track's *terminus*. Note from the enlarged inserts that these terminal sections are commonly characterized by deformation structures and fractures systems that resemble inverted cones. This cone-in-cone structure is seemingly a characteristic, yet poorly understood mode of failure for aerogel, presumably at high strain rates. The very tip of the terminus is often curved, as the last few cones are misaligned. Projectile residue, if present, typically resides in undeformed host aerogel at a modest distance from the last cone structure.

Figure 17 shows a number of tracks, arranged by decreasing L/D and including select side views to provide a sense for the morphologic diversity (*e.g.*, throats and main cavities) of individual tracks. Note the relatively straight walls and constant tapering of the entire feature for most tracks of $L/D > 30$ (*i.e.*, for most of the longer tracks). In such continuously tapering cases, it is not possible to differentiate between the main cavity and the stylus. Such tracks are generally characterized by a relatively short throat, reaching maximum feature diameter very close to or at the surface of the aerogel. As throat length gets longer than D , the cavity walls tend to become curved, forming modestly and distinctly bulged cavities that merge into the stylus in a progressively more abrupt fashion. Ultimately, the main cavity may maintain a constant diameter over a relatively long distance, resulting in distinctly cylindrical geometries that occupy progressively longer portions of the main cavity.

In an idealized sense, cavity shape changes continuously from slender, straight-walled cones, to bulged forms, to cylindrical cavities. In contrast, the stylus remains a relatively invariant, needle-like structure. Distinctly bulbous and cylindrical main cavities display progressively more abrupt diameter changes as the main cavity transitions into the stylus, with some cylindrical cavities approaching almost discontinuous steps. Clearly, such cylindrical cavities are transitional to deep pits, the latter lacking the needle-like stylus and terminating in blunt-nose fashion (see below).

Note that the concept of an L/D has limited meaning in the case of classical penetration tracks. The diameter D may refer to wedge-shaped, bulbous or cylindrical cavity geometries with the length of the stylus substantially controlling the total track depth (L). The distinction among various sub-classes of tracks is based on the detailed shape of the main cavity, rather than on specific L/D measurements. The concept of L/D becomes meaningful only in the context of pits and other, significantly shallower structures present on ODC.

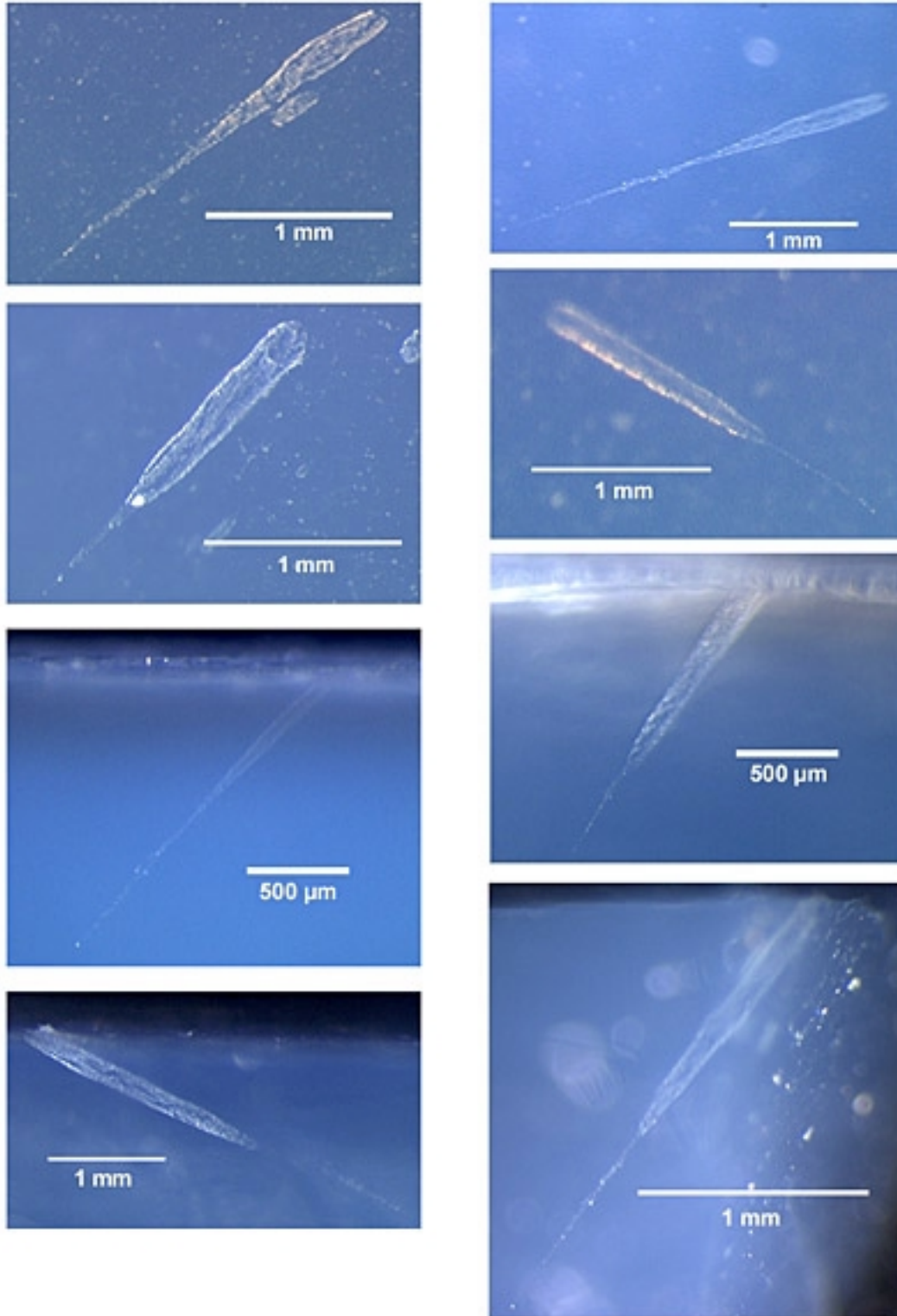


Figure 17. Typical tracks observed in ODC aerogel. Note some modest differences in the morphology of the main cavity, ranging from slender cones to slightly bulged.

The significance of the subtle morphologic changes described above and illustrated in Figures 16 and 17 is poorly understood at present and attests to a wide range of initial impact conditions. Based on experimental impacts into highly porous media such as sintered alumina (Werle *et al.*, 1981) or styrofoam (Tsou, 1990), total penetration depth systematically increases up to some threshold velocity, beyond which it decreases again. However, the total volume of the track continues to systematically increase with increasing velocity, even beyond the threshold, at least for experiments using styrofoam at impact velocities as high as 7 km/s (Tsou, 1990). This implies that the main cavity diameter must increase at the expense of penetration depth. All of the above experimental series were conducted into porous targets with densities $> 0.1\text{g/cm}^3$. There is no experimental confirmation for such a velocity-dependent threshold of L/D for the lower density aerogels employed by ODC, at least at velocities as high as 7 km/s (Hörz *et al.*, 1997), yet it may very well exist at $V > 7$ km/s. We will return to the existence of such a threshold velocity after the description of pit features, which will figure prominently in such considerations.

Classical penetration tracks, as illustrated in Figures 15 - 17, are very common in the ODC aerogel, if not the most common impact feature type. However, they are generally limited to small sizes (< 5 mm in length). The longest track observed on ODC was ~ 15 mm long with an angle of incidence of some 45° , and was terminated by the aluminum Interface Plate. This was the only track on ODC to completely penetrate the aerogel; the second longest track was ~ 7 mm long. Typically, each aerogel tile contains tracks that are readily seen with the unaided eye. The macroscopic inspection of all tiles yielded a total of 86 tracks > 3 mm in length for the entire ODC, while small numbers of tracks 1 - 3 mm in length, and numerous tracks < 1 mm in length are seen on every tile under the microscope. In addition, microscope inspection reveals that most tracks possess some form of impactor residue at their termini, substantiating that the aerogel on ODC did capture hundreds of impactors large enough ($> 5 \mu\text{m}$) to be analyzed with modern analytical instruments.

As illustrated in Figure 18, it is not unusual to have *bifurcated tracks* or tracks that possess multiple styluses, which attest to the fragmentation of the penetrating impactor. The bifurcation or splitting of the projectile to produce two or more stylus-features typically occurs at the end of the main cavity. Furthermore, the longest stylus does not necessarily contain the largest projectile fragment. Small and relatively dense fragments may penetrate more deeply or individual fragments may possess faster velocities than the main mass.

An unusual set of tracks, all confined to the rearward-facing ODC surfaces (*i.e.*, Tray 2), needs mentioning. Some of the tiles in this tray contained distinct *clusters* of tracks as illustrated in Figure 19, which is a mug shot of tile 2E01. In general, the clusters of tracks are of sufficient size and quantity to be seen with the unaided eye. Each cluster may be composed of tens, if not hundreds of (small) tracks, all of grossly similar shapes, and all exhibiting identical azimuthal orientation and identical, relatively shallow angle of incidence, $\sim 25 - 30^\circ$ relative to the tile surface/local horizontal. The spatial density of tracks $> 500 \mu\text{m}$ in length occasionally exceeds 10 tracks/ cm^2 in such clusters, with the cluster typically a few cm across, thereby occupying a (small) fraction of the host tile(s). The cluster illustrated in Figure 19 is the largest observed. The density of tracks within a cluster drops off rather sharply, if not abruptly, into the surrounding aerogel. Higher magnification views of some clustered tracks can be seen in

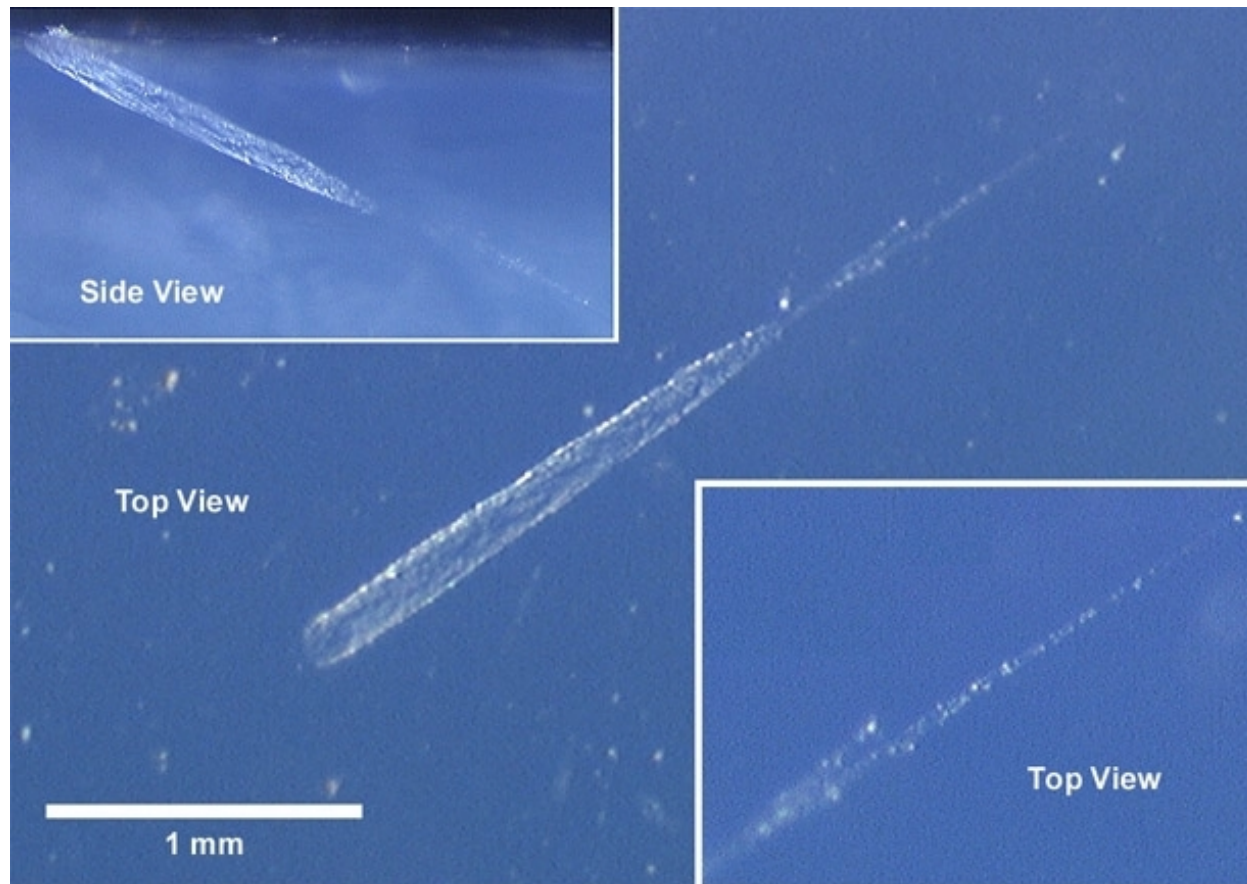


Figure 18. Example of a bifurcated track caused by the fragmentation of the penetrating impactor. Note that the shorter track contains the larger residue.

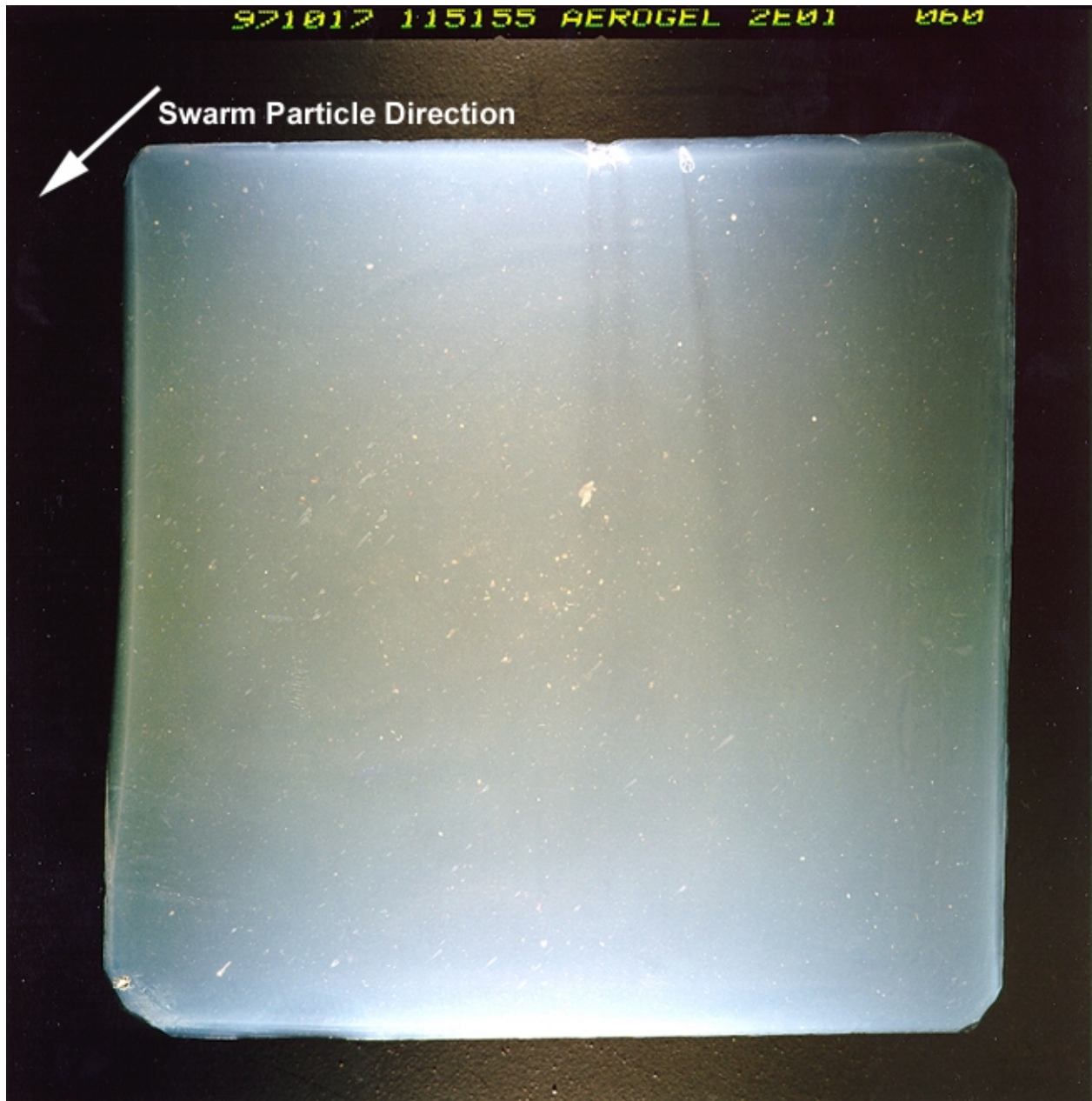


Figure 19. Tile 2E01 that contained the largest cluster of tracks, all having identical azimuthal orientation, as well as a modest inclination angle ($\sim 25^\circ$) from the local horizontal.

Figure 20. Note their limited range of shapes, their constant azimuthal direction in plan view (top panels), and their constant inclination/trajectories in cross-section (bottom panels). These images also illustrate that any cluster may contain tracks of vastly different sizes.

A total of five prominent clusters were observed on Tray 2 of ODC, with the two largest clusters located on neighboring tiles 2D01 and 2E01. However, these two clusters are distinctly separate and do not extend across the tile boundaries; they are two distinct features. The

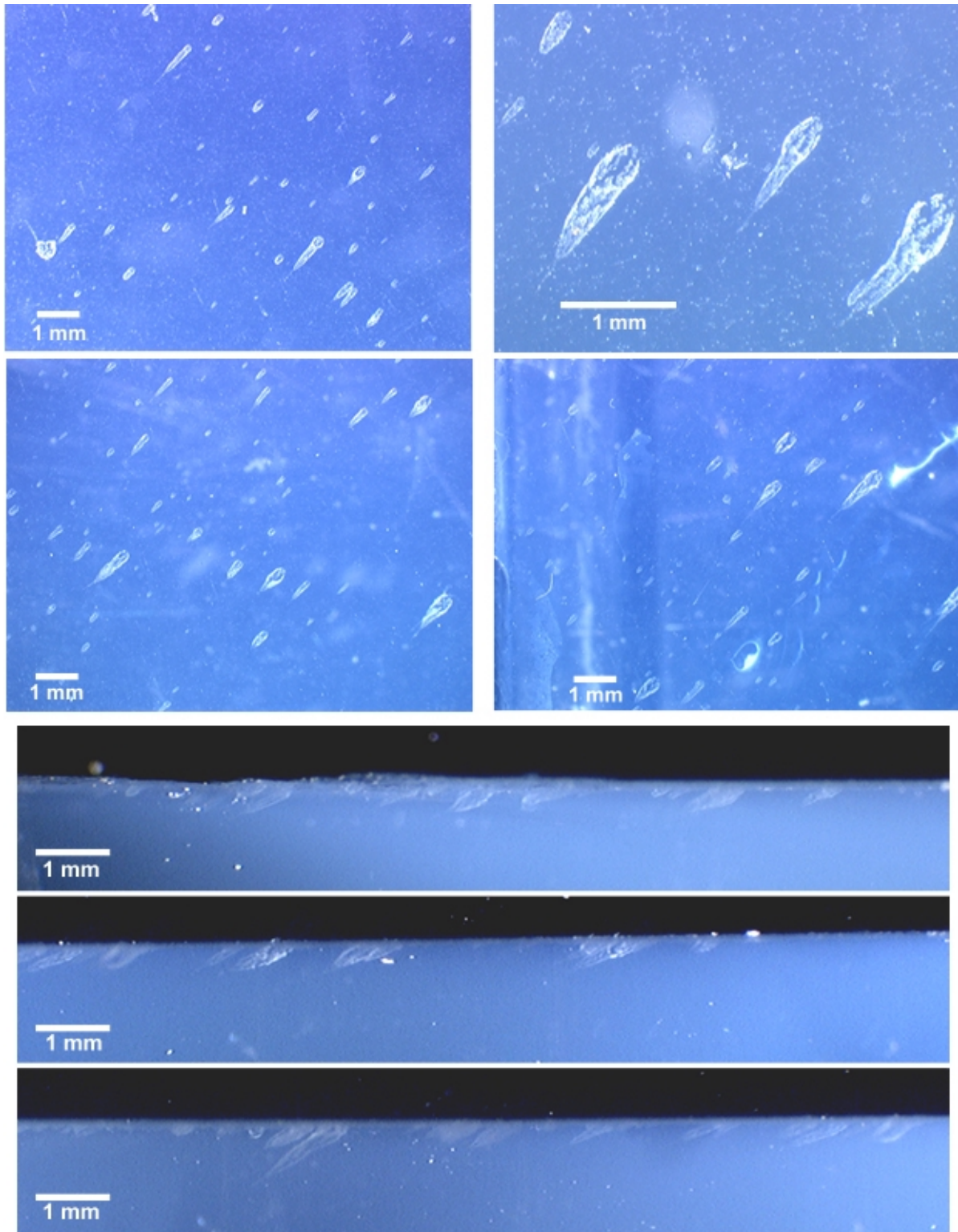


Figure 20. Detailed views of the swarm event in plan view and cross section. Note the high spatial density ($\gg 10$ tracks/cm²) of tracks and their variable lengths, the latter indicative of widely variable impactor sizes. The main cavities of these tracks are fairly constant, with modestly to distinctly bulbous cavity geometries.

remaining clusters seem randomly distributed. The observed clusters are distributed in an irregular fashion over the entire Tray 2 surface, with individual patches occupying only a small fraction of their respective host tiles.

However, there are numerous, individual tracks on most Tray 2 tiles that exhibit features with similar shapes, orientation, and inclination as those associated with these clusters. The sheer frequency of features with identical trajectory elements leaves little doubt that they are associated with the clusters. Evidently, the clusters and the geometrically identical, yet isolated tracks were produced by a distinct cloud of impactors that must have originated locally, most likely as ejecta from an impact on some MIR surface. This particle cloud had a distinctly heterogeneous mass distribution, ranging from dense lumps of particles to more dispersed, individual fragments. The distribution of particle size or mass within this cloud was also highly variable, as track lengths vary by more than an order of magnitude. We refer to this particle cloud and its tracks as the “swarm” or “swarm event” throughout the rest of this report.

Pits

In comparison to tracks, pits seem anomalously shallow for hypervelocity impacts, with typical L/D ratios of 0.5 – 2. The shallowest members are almost hemispherical in shape, yet the deeper features have long, vertical walls, resulting in distinctly cylindrical cavities. All terminate with relatively blunt noses and lack the telltale, slender stylus associated with tracks. Generally, they contain no macroscopic and microscopic evidence of impactor material. Indeed, the lack of any discoloration renders them exceptionally transparent and clear, one of their most outstanding attributes. Such features have no experimental analog to our knowledge, yet we note that they were also found in aerogels that were exposed prior to ODC on the *EURECA* satellite (Brownlee, 1994; personal communications, 1998) or on the Shuttle (Westphal, personal communications, 1998). In particular, Brownlee seemed puzzled by such features, as none contained detectable projectile materials, neither under the microscope nor via SEM-EDS. Unfortunately, none of these earlier observations were described in the open literature.

Typical plan views and cross sections of pit structures can be seen in Figure 21, with additional examples, showing their variety, visible in Figure 22. A first-order resemblance with impact craters in dense target media is suggested for some of the shallower features, yet there are also substantial differences, the reason why we refer to these shallow structures as pits and not as craters. For example, even the most crater-like, hemispherical pits lack a raised rim. Furthermore, many of these features exhibit radial fractures (*i.e.*, spike-like features) around their periphery, the reason why Westphal (personal communications, 1998) refers to them as “hedgehogs”. In addition, they lack any concentric spall zones and fractures typical of craters in brittle materials, such as glass (*e.g.*, Schneider *et al.*, 1990). The aspect ratio of pits is typically $1 > L/D < 5$. This contrasts with aspect ratios for typical hypervelocity craters in space-exposed aluminum ($L/D \sim 0.5 - 0.6$; Love *et al.*, 1995) and $L/D \sim 0.2 - 0.3$ in typical silicates and rocks (Gault, 1973). Compared to craters, even the shallow ODC pits are fairly deep. The long cylinders illustrated in Figure 21 are highly unusual for hypervelocity impacts. However, as illustrated in Figure 22, shallow and deep structures are clearly transitional, thus justifying the term “pit” as a single term for this entire class of features.

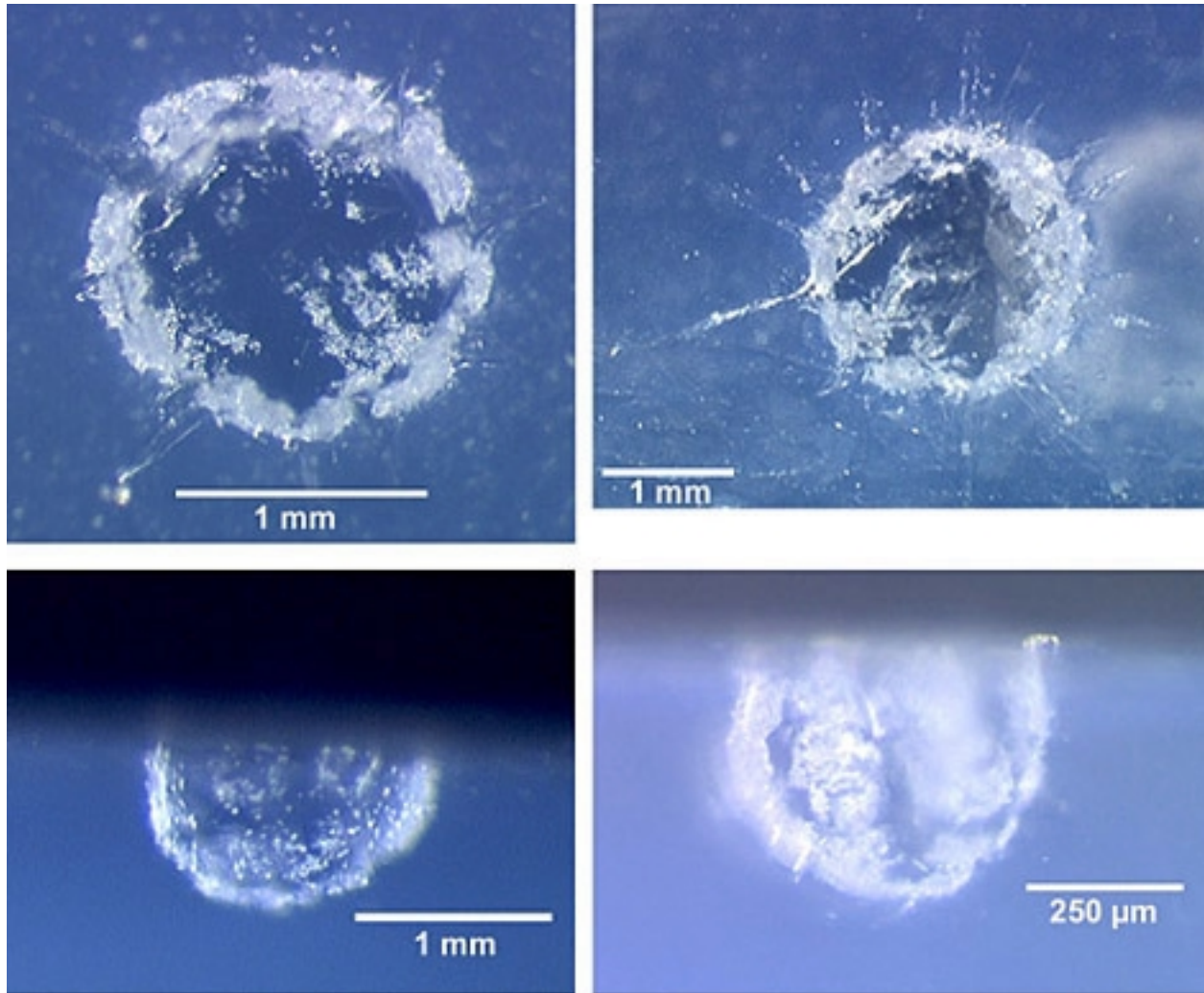


Figure 21. Examples of typical pit features in plan view and cross section. Note their relatively shallow nature, the lack of a raised rim, and the lack of concentric fracture systems typical of spall phenomena in glass targets. The structure on the right side has spike-like, radial fractures. Such impact pits in aerogel have no experimental analog.

The interior surfaces of pits (*i.e.*, bottoms and walls) differ from that of tracks in that they tend to be highly transparent. The main cavity walls, especially the deeper portions, of most tracks are modestly opaque and of a mottled appearance, resulting from mechanically deformed, finely crushed aerogel that scatters light. Styluses tend to exhibit similarly opaque walls that commonly grade into the cone-in-cone structure. In fact, it is these observations of the stylus that suggest that this material consists of finely crushed aerogel. In contrast, pit features tend to lack this modestly opaque, mottled zone and, as a result, are highly transparent. Many pit walls are somewhat undulous in appearance, and occasionally contain prominent, bulbous promontories. Similarly transparent walls are observed in the main cavities of some tracks as well, especially those with cylindrical shapes. We interpret these highly transparent, modestly undulous surfaces as evidence of melting, yet we do not imply the presence of a continuous melt liner. The aerogel may merely have shrank and contracted in response to elevated temperatures. Dedicated SEM studies are needed to characterize the distinctly bimodal appearance of cavity surfaces, and to verify the current interpretations of finely crushed versus molten aerogel.

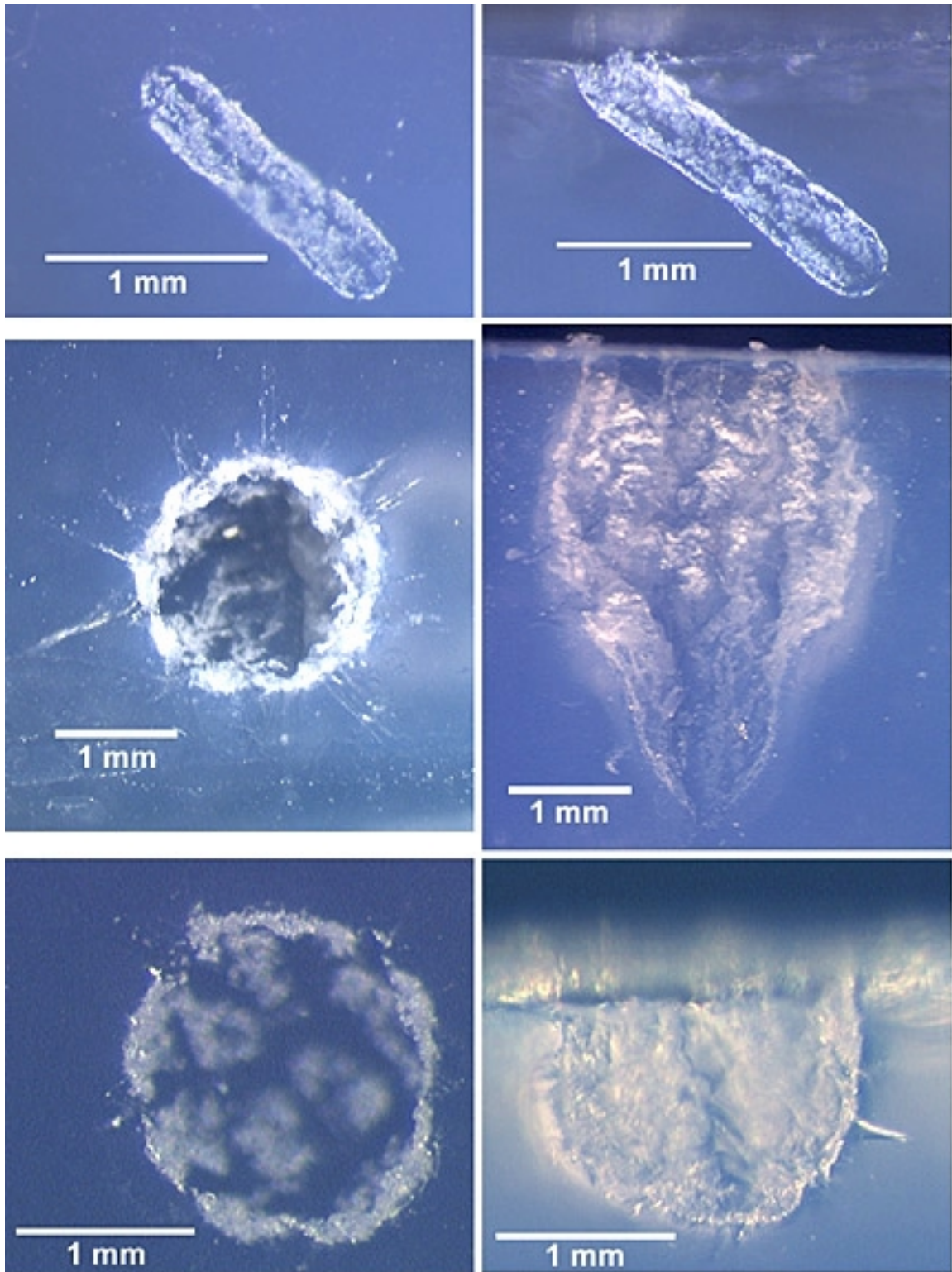


Figure 22. Plan view (left) and cross-sections (right) of three pits, including a deep cylindrical cavity (top), a stubby example (middle), and an essentially hemispherical pit (bottom).

We note that the entrance hole of many pits is smooth and contains small-scale promontories, sometimes of a beaded appearance, all consistent with if not suggestive of melting.

Significantly, pits generally contain no obvious projectile residues, even when viewed under the microscope. Generally, the feature walls and bottoms do not exhibit the slightest hint of discoloration, a remarkable observation if the above interpretation of molten pit walls is correct. Typically, impact melts found in the interior of experimental craters (e.g., Hörz *et al.*, 1983; Gwynn *et al.*, 1996), on metal substrates flown on LDEF (Bernhard *et al.*, 1992), or on lunar rock and mineral surfaces (e.g., Schaal *et al.*, 1976) are dark colored, reflecting Fe and other metals present in the impactors. By comparison, the aerogel pits are remarkably colorless and transparent. Brownlee (personal communications, 1998) made identical observations and was somewhat frustrated that none of the pits retrieved from *EURECA* yielded analyzable residue via SEM-EDS methods; we describe similar results below. However, the spike-like cracks surrounding some of these pits do, on occasion, contain dark materials that has not been analyzed to date, and which may be impactor residue.

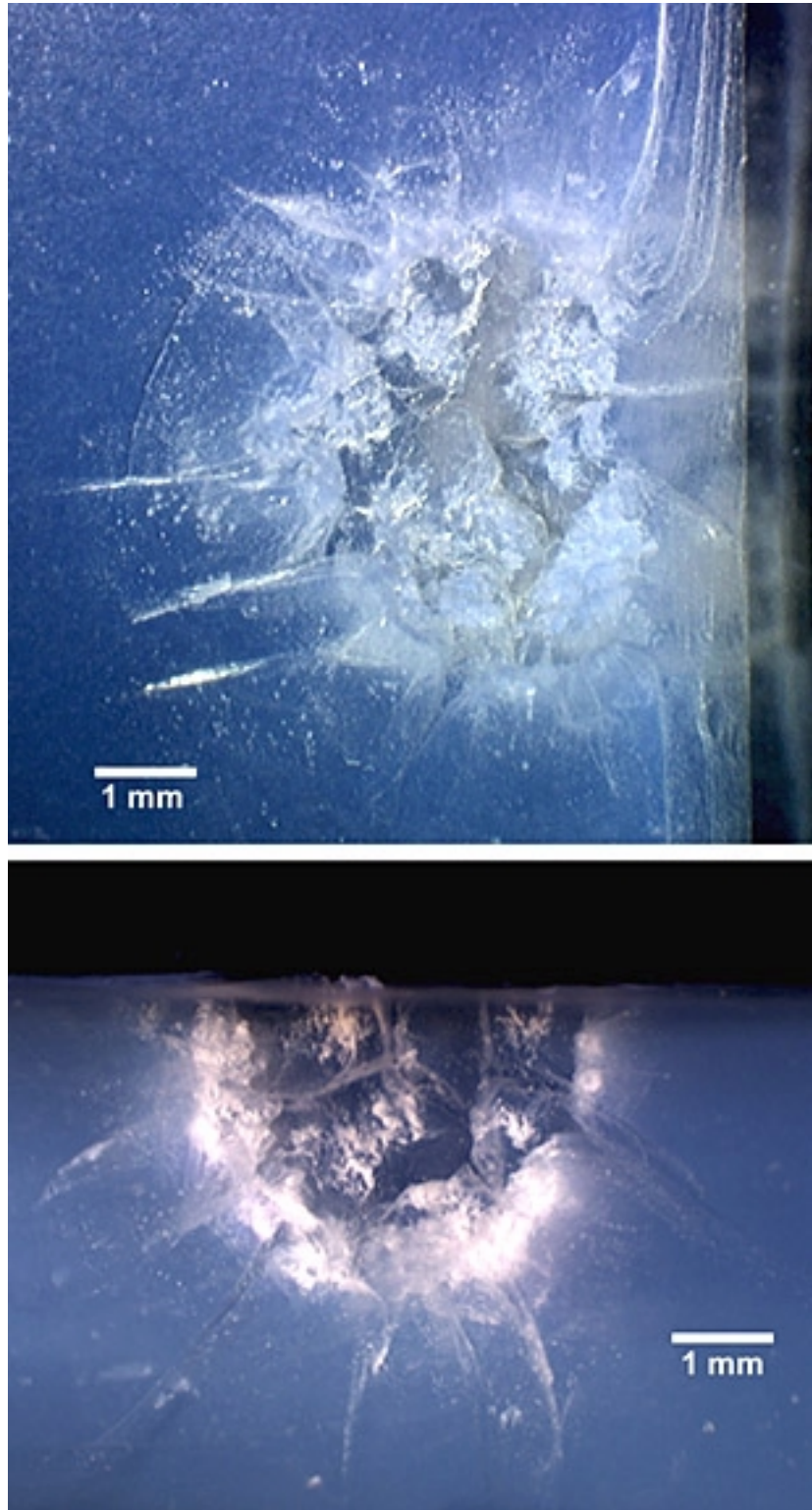


Figure 23. Largest impact feature observed on ODC, which happens to be a pit whose growth was unfortunately affected/terminated by the ODC Assembly Frame (see Figure 13). Top: Plan view. Bottom: Cross section

Another important characteristic of pits is their apparent size dependency. Most of the largest impact features (> 5 mm in L or D) found on the ODC collectors are pits. The largest impact feature to occur on ODC is a pit ~ 9 mm across (Figure 23 and tile 2B01 in Appendix A). Despite its large diameter, this event barely penetrated ~ 6 mm into the aerogel (see cross section in Figure 23) and has an $L/D < 1$. Another exceptionally large pit occurs on tile 1C04. Its entrance-hole diameter is modestly smaller than that shown in Figure 23, yet it is ~ 8 mm deep and the associated radial spikes were terminated by the Interface Plate, producing some discoloration of the plate, yet no physical damage/indentation. It is the only pit feature observed on the entire ODC experiment that (barely) penetrated the entire aerogel layer, despite a fair number of pits that have diameters > 5 mm.

The origin of pits is poorly understood, as they do not have an experimental analog at impact velocities as high as 7 km/s. Superficially, the shallow, hemispherical pits resemble structures produced in aerogel by modestly compressed cocoa-powder at 6 km/s (Hörz *et al.*, 1997). This suggests that shallow pits could be the result of low-density, possibly very fluffy and friable impactors. However, the experimental pits (Figure 24) were loaded with projectile residue, as evidenced by the brown color of their interior surfaces. The absence of impactor residue is the strongest argument against a low-velocity origin of the ODC pits.

Furthermore, impacts of low-density, extended projectiles (*i.e.*, collisionally fragmented glass spheres; Hörz *et al.*, 1997) result in relatively stubby aerogel cavities that are the composite of numerous small impactors. However, many large, individual fragments penetrate beyond the main cavity producing parasitic tracks (Figure 24). The absence of similar parasitic tracks around the ODC pits is significant and argues against fluffy impactors at modest velocities. Even the shallow, hemispherical ODC pits have no experimental analog, much less the deep cylindrical structures.

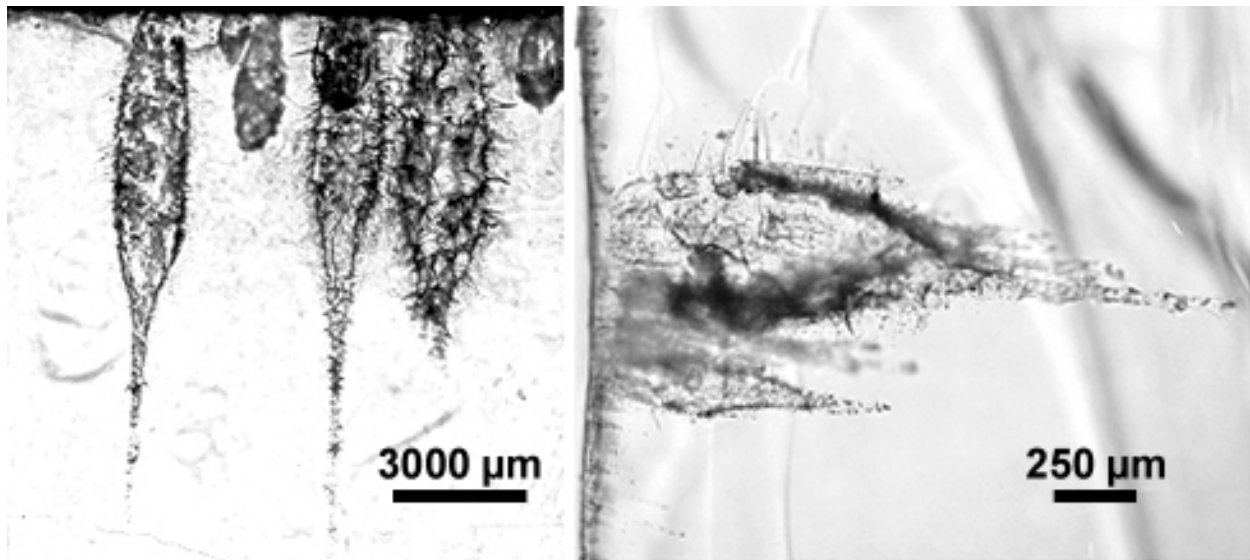


Figure 24. Experimental impact features in 0.02 g/cm^3 aerogel. In the left-hand image are impacts at 6 km/s of loosely consolidated clumps of cocoa powder, some composed of pure cocoa (short features) and some containing solid-aluminum spheres of $50 \text{ }\mu\text{m}$ diameter that penetrated beyond the main cavity to produce a stylus. On the right are impacts resulting from a collisionally fragmented glass sphere resulting in stubby cavities on many of the parasitic tracks.

We are confident that shallow and deep pits are transitional in nature. More importantly, we suggest that tracks and pits are transitional, as well. A few cylindrical cavities exist that possess a blunt-nosed terminus, from which a single stylus emerges, as illustrated in Figure 25. Such structures seem crucial to understanding the transitional relationship of tracks and pits. By definition, the stylus requires that the entire feature be classified as a track, yet the properties of the main cavity seem to match all the characteristics of pits. This transitional evolution of track geometries is schematically illustrated in Figure 26. Slender, gradually tapering cavities merge into bulbous cavity shapes, the latter also developing progressively more distinct stylus features at depth. As the longitudinal extent of the bulbous cavity increases, increasingly larger portions of the cavity become cylindrical in shape. With increasing cylinder length, the transition to the stylus becomes increasingly more abrupt. Ultimately, the long cylinders develop a distinctly blunt-nosed bottom from which a relatively modest-sized stylus emerges. Although we have no quantitative measurements, the relative volume of the main cavity increases throughout this evolutionary sequence relative to that of the stylus, the latter becoming especially small when cylindrical cavities develop the blunt noses. Ultimately, the stylus disappears and a deep, cylindrical pit remains that becomes progressively more shallow, yielding pits of increasingly smaller L/D , until hemispherical geometries are approached ($L/D = 0.5$).

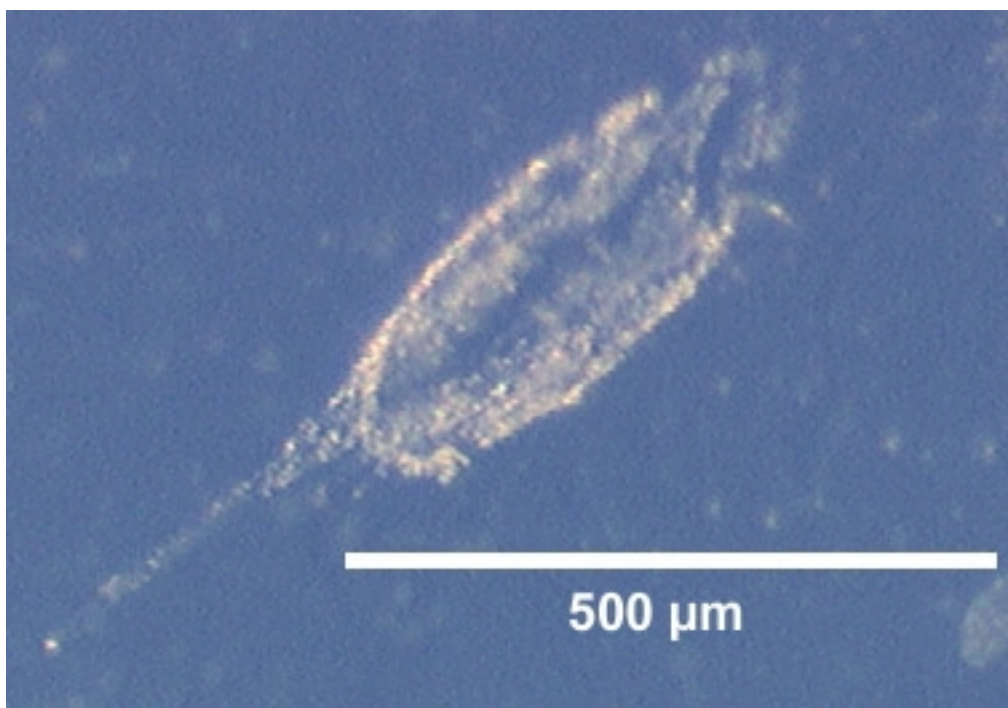


Figure 25. Relatively blunt nosed, cylindrical cavity associated with a modest size stylus. Such features seem critical for illustrating a morphologic continuum from tracks to pits.

These highly variable morphologies reflect a wide range of initial impact conditions, foremost impact velocity and/or projectile physical properties, especially density. We favor the view that impact velocity plays the dominant role, rather than the projectile's physical properties. This suggestion rests - in large measure - on experimental evidence, as scant and incomplete as it may be. In analogy to the impact experiments of Werle *et al.* (1981) and Tsou (1990), there must be a threshold velocity, even for very low-density aerogels, beyond which absolute track depth



decreases, producing main cavities of relatively large diameters and volumes, and leading to decreased L/D . Such systematic, velocity-dependent changes in L/D are also observed for genuine impact craters. Craters produced by glass projectiles at 1 - 2 km/s in aluminum targets are relatively deep compared to those at 6 - 7 km/s (Murr *et al.*, 1998; Hörz, *et al.*, 1995). Experiments related to the development of orbital-debris shields also reveal that low-velocity impactors penetrate with greater efficiency than those at high velocities (*e.g.*, Christiansen, 1995). The reason for this behavior is that the impactor deforms plastically (or melts and vaporizes at still higher velocities) at some threshold velocity and thus, deforms with ease, leading to decreased penetration efficiency (see also Gault and Wedekind, 1977; Murr *et al.*, 1998).

We invoke an analogous behavior in the case of aerogel targets with the threshold velocity being well beyond light-gas gun capabilities (> 7 km/s) where shock stresses and specific energy will exceed the melt temperature, if not the vaporization threshold. It is our view that the continuously tapering tracks reflect modest-velocity impacts, short of substantial projectile melting, akin to their experimental analogs. Increasingly more bulbous cavities suggest progressively larger degrees of projectile deformation (possibly melting?) and associated increases in the effective cross section of the impactor. The onset of cylindrical cavity sections and their typically highly transparent, glazed walls delineates elevated thermal conditions, which we equate with melting, either by direct shock or assisted by ablative melting, most likely both (Anderson and Ahrens, 1994). However, part of the impactor remains unmolten to form the stylus; the surviving cores or fragments are substantially decelerated, making them into highly efficient penetrators at modest velocities. Projectile residues recovered at the end of some stylus corroborate the unmolten nature of such fragments. We have never encountered a completely molten impactor residue at the terminus of a track, neither in experiments nor on ODC. The morphology of the stylus and the presence of unmolten projectile residues suggest that it is a low-velocity penetration feature, common to all unmolten cores or fragments of particles that were decelerated to below some (unknown) threshold velocity.

By the time the main cavity becomes increasingly cylindrical, the cavity walls assume a highly transparent character, as if molten. This transition is complete for deep, blunt nosed cavities that are invariably also of cylindrical shape. Some of these cavities may have a modest stylus, depending whether some small projectile fragment survived or not. Obviously, thermal effects dominate the development of these cylindrical cavities, and cause the cavity walls to melt or shrink. We speculate that these pits have largely formed by an expanding vapor cloud that is sufficiently dense and hot that it displaces and thermally erodes the aerogel, thus forming a relatively cylindrical cavity along the penetration path. The higher the velocity, the more efficient the production rate of such vapors near the surface, effectively resulting in near surface bursts that produce the very shallow, hemispherical pits. Note that most of the expanding vapor could originate from the aerogel target itself. This vapor may entrain and ultimately eject the molten, if not vaporized impactor to yield transparent pit interiors that lack even traces of impactor residues.

This velocity dependent scenario for the morphologic evolution of impact features in the ODC aerogel is largely derived from the two end-members, the continuously tapering track, which contains copious amounts of impactor residue, and the shallow pit that typically contains none. A number of considerations combine to favor velocity as the dominant factor in this evolution, as opposed to the projectile's physical properties. First, none of the cylindrical cavities, much less the shallow pits, can be experimentally reproduced at velocities as high as 7 km/s, and including low-density ($\ll 1 \text{ g/cm}^3$) and low-velocity (3 km/s) projectiles (Hörz *et al.*, 1997). Second, experimental evidence in highly porous targets suggests the existence of a threshold velocity, beyond which the cavity diameter increases at the expense of penetration depth (Werle *et al.*, 1981; Tsou, 1990). Lastly, general shock considerations mandate a systematic progression from melting to vaporization phenomena with increasing velocity. The latter is amply demonstrated by impact craters in space-exposed, non-porous materials, such as aluminum or gold substrates exposed on LDEF; ~ 50% of these craters did not reveal any impactor residue at the sensitivity level of SEM-EDS methods (Hörz *et al.*, 1993). We consider the pit-structures in aerogel to be equivalent to craters in non-porous targets that contain no projectile residue, both structures primarily the result of impact at very high velocities.

If the projectile's physical properties were largely responsible for the transitional nature of track and pit morphologies, one would assign the very deep, continuously tapered tracks to high-density impactors, and the shallow structures to the low-density extreme. Note that the highest peak stresses and melting or vaporization phenomena in the target would be associated with the tapered tracks, rather than with the shallow pits, in such a scenario. It seems unlikely that all low-density impactors were consistently above the threshold velocity for complete vaporization, as none of them left detectable residues in the pits. We would expect an abundance of parasitic tracks associated with friable, low-density impactors at modest encounter velocities, akin to experimental analogs. As a consequence, the velocity dependent scenario seems much more consistent with the observational evidence.

Regardless, pit structures contain little or no impactor material(s). This is an important finding as it suggests a practical limit for the utility of aerogels in the capture of hypervelocity particles. While the threshold velocity for successful capture of unmolten particle residues with aerogel is undoubtedly much higher than that for non-porous target media, there will be a

velocity controlled cut-off. Future experiments must address this limit, either by suitable analog experimentation at modest velocities, or by improvement of current launch technologies to achieve much higher projectile velocities, ideally approaching 20 km/s.

Shallow Depressions

This category of impact feature differs from tracks and pits and can be subdivided into two subclasses, depending on the physical state of the projectiles at the time of impact: (a) solid flakes and (b) liquid droplets. Both impactor types are man-made waste products (as revealed by SEM-EDS analyses; see below) that co-orbit the MIR station, resulting in encounter velocities as low as a few meters per second and producing relatively shallow depression upon impact. Typically, these depressions are shallower than pits, possessing $L/D < 1$.

Flakes - This subclass exhibits L/D ratios < 1 , commonly < 0.2 .

They were termed “flakes” because many such features contain white to brownish colored, irregular shaped, platy materials within the depression. In the extreme case, some flakes have merely stuck to the aerogel, with parts of the flake protruding above the aerogel surface. The damage caused by most flakes is a shallow depression of irregular outline that contains a crushed layer of aerogel at the bottom, as illustrated by an especially large example in Figure 27; additional examples are illustrated in Figure 28. The copious amounts of impactor material in these shallow depressions, combined with a layer of crushed aerogel, clearly distinguish this class of structures from the transparent hypervelocity pits. Most objects that appear as white dots in the mug-shot photographs (Appendix A) represent such flake impacts, with most tiles containing a number of such features.

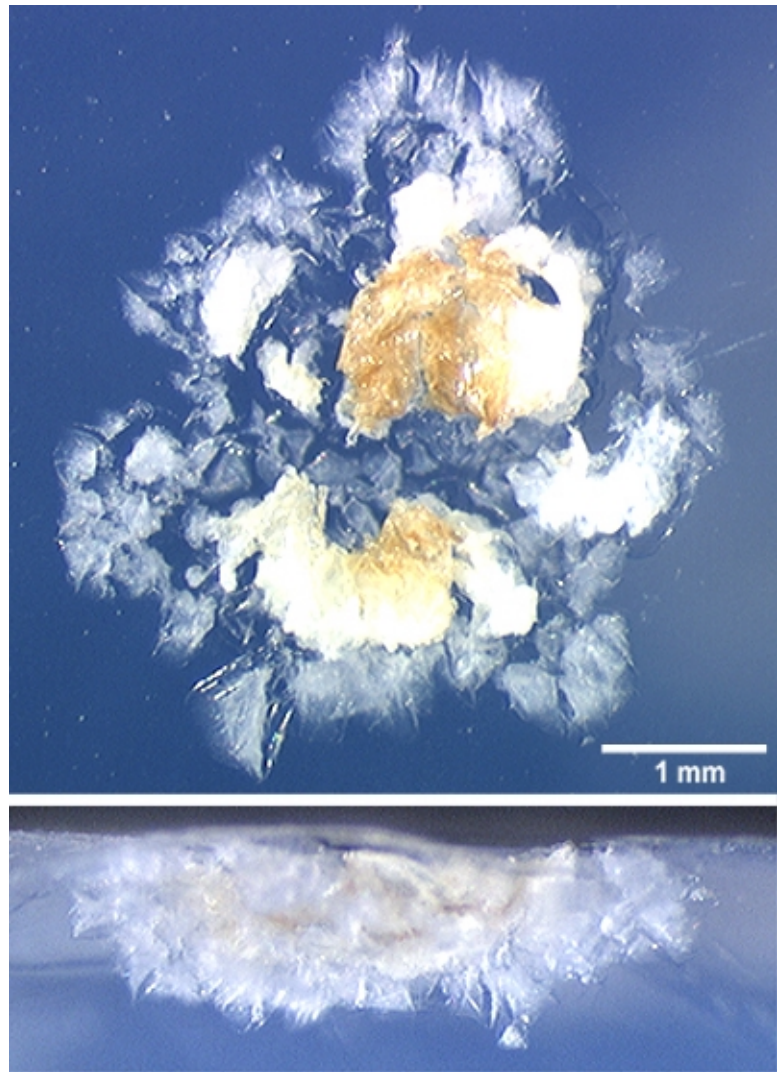


Figure 27. Unusually large flake impact in plan view and cross section. Note the highly irregular outline and the shallow depth of penetration. The initial flake actually broke up into a number of pieces, some displaying a distinctly honey colored hue. The relatively thin layer of highly crushed aerogel suggests a low-encounter velocity.

Their shallow nature, and the fact that some flakes seem to have barely penetrated the aerogel, suggests they result from exceptionally low encounter velocities, indicative of co-orbiting materials.

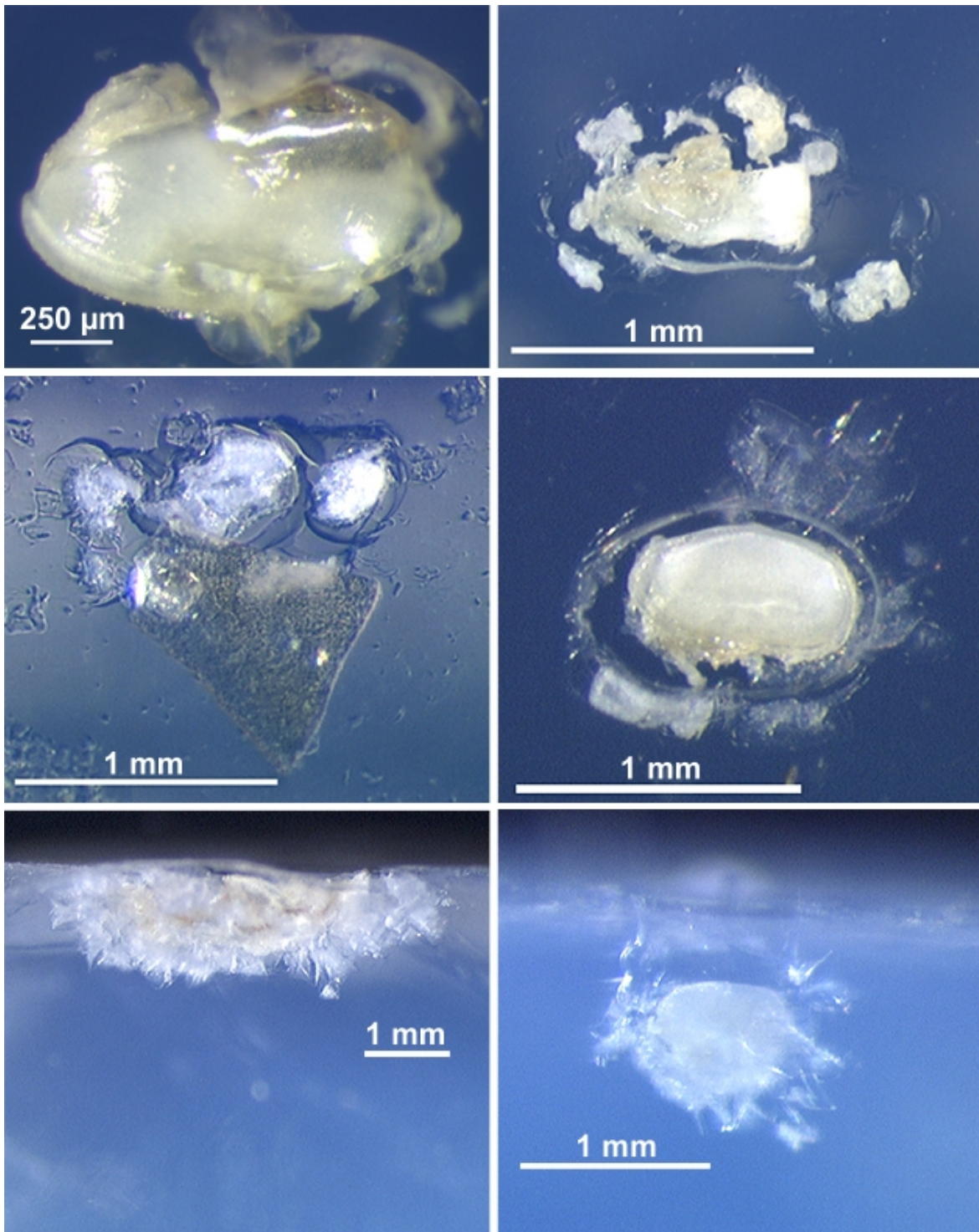


Figure 28. Additional examples of flake impacts, some having rounded and wetted appearances suggesting a mixture of solids and liquids (see text).

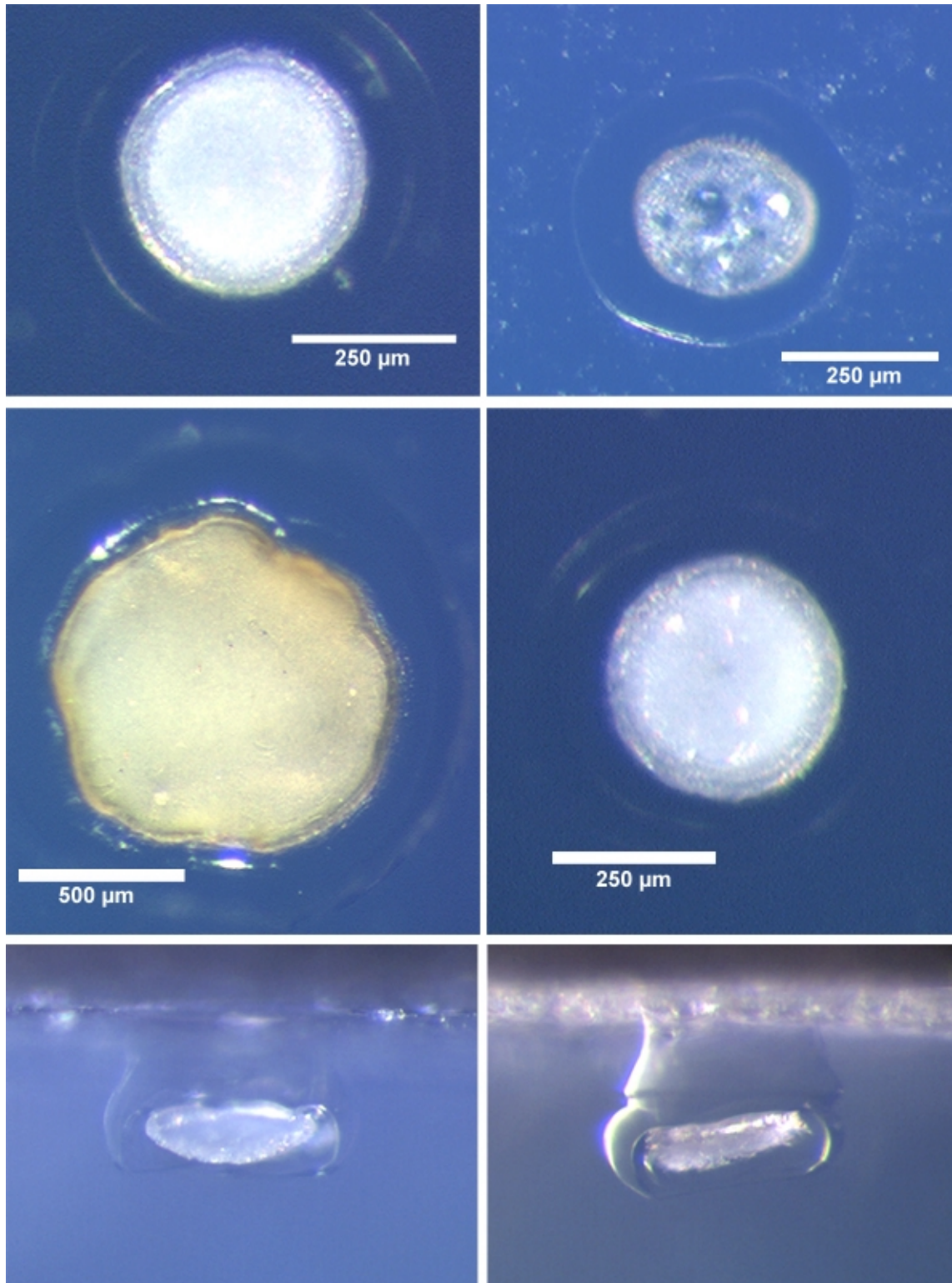


Figure 29. Typical examples of droplet impacts in plan view (top four panels) and cross section (lower panels). Note that the petri-dish shaped bottoms contain a distinct deposit that commonly has concentric qualities, especially towards the edges.

Liquid Droplets – Akin to flakes, these features are relatively shallow in depth, generally $L/D < 2$. Typical examples can be seen in Figure 29. Unlike the flakes, however, this subclass of feature tends to be small in diameter, generally < 1 mm across. Macroscopically they are white specs, akin to flakes, and it takes the microscope to recognize them as a separate class of impact feature. Several characteristics support the conclusion that these depressions were caused by liquid droplets of low-encounter velocity. First, they are highly circular in plan view, totally unlike the irregular flake impacts. Second, there is no fracturing, cracking, crushing or other disturbed aerogel, unlike all other impact features. The relatively large entrance holes are free of mechanical defects, and thus, hard to spot in plan view. Below the aerogel surface, the feature walls often undercut the entrance hole expanding outward to a bulbous, circular bottom that has the shape of a petri-dish (bottom frames of Figure 29). Such depressions differ dramatically from all other impact features, primarily by their regular shapes and lack of aerogel deformation. Third and most importantly, the circular bottoms contain white to tan material that has distinctly concentric color variations and micro-fractures resembling dried mud cracks. There is little doubt that this is a deposit formed *in situ* by precipitation from some liquid. Preliminary compositional analysis of the precipitate, as detailed below, identifies these deposits as human waste.

It is important to note that the PPMD and POSA experiments also observed round and even elongate, splash-like deposits on a wide variety of surfaces (Kinard, 1998; Pippin, 1998). Thus, there is independent evidence from other MEEP experiments for the existence of liquid droplets. Their detailed spatial distribution pattern on the POSA I instrument and its orthogonal container walls, combined with geometric shielding considerations, suggests the docked Shuttle as the most likely source of this material (Pippin, 1998). The docked Shuttle conducted six wastewater dumps while the MEEP experiments were exposed on MIR, each dumping ~ 20 gallons of liquid waste (Visentine, personal communications, 1998).

Note that some of the flake impacts have substantially rounded portions, either in plan view or cross section (see Figure 28), akin to the much more regular droplet features. This appears consistent with variable mixtures of liquids and solids, all derived from Shuttle's waste management system, and resulting in co-orbiting particles of low-encounter velocities.

Relative Frequencies

The above descriptions of impact features in space-exposed aerogel included microscopic evidence, if not SEM-EDS analyses, primarily to introduce their morphologic characteristics and to support some of the interpretations. We now return to the first order, macroscopic survey of all ODC tiles that was to obtain a complete inventory of all features > 3 mm in diameter or depth, which was conducted immediately after harvesting of all of the tiles. Although distinct classes of impact features were obvious upon opening of the MEEP containers, the detailed interpretations offered above represent our present understanding and were not available and/or appreciated at the time the macroscopic survey was conducted. For this reason, we derived only three types of features during the initial macroscopic survey: (a) tracks, (b) pits, and (c) flakes. Within the current interpretative framework these features now represent (a) low-velocity impacts (b) very high-velocity impacts, and (c) low-velocity encounters with human waste products, both solid and liquid.

Table 1. Absolute and relative frequency of genuine tracks, pit-type features and flake-depressions > 3 mm that were captured by ODC aerogel of a cumulative surface area of ~ 0.32 m² per tray. The differences between Tray 1 and Tray 2 are given by the 001/002 ratio.

| | Tracks | Pits | Flakes | Total |
|----------------|-------------|-------------|-------------|------------|
| ODC 001 | 23 | 33 | 156 | 212 |
| Percentage | 10.8% | 15.6% | 73.6% | 100.0% |
| ODC 002 | 63 | 41 | 35 | 139 |
| Percentage | 45.3% | 29.5% | 25.2% | 100.0% |
| 001/002 | 0.37 | 0.80 | 4.46 | |

The quantitative results of our first-order, macroscopic survey are summarized in Table 1 and illustrated in Figure 30. A first-order observation is that there is a higher frequency of flake and droplet features on Tray 1 compared to Tray 2, corroborating POSA’s conclusion (Pippin, 1998) that most of this debris was derived from the direction of the docked Shuttle. The relative frequency of pit features is similar on both surfaces. We realize that this appears inconsistent with a velocity-dependent origin of these structures, because the average encounter velocity of forward and rearward facing surfaces should differ dramatically on a non-spinning platform, with much higher velocities prevailing on ram-pointing surfaces (*e.g.*, Zook, 1991). However, the pinhole camera of the co-located PPMD experiment reveals considerable deviation of Mir from the ideal of a non-spinning platform. As a consequence, we consider similar pit frequencies on Tray 1 and 2 to be consistent with a velocity-related origin. Genuine, carrot-shaped tracks are about a factor of two higher on Tray 2 than on Tray 1. Although we excluded the obvious clusters of swarm tracks from these frequency data, we had no quantitative means to exclude non-clustered, isolated members of the swarm from the frequency statistics for tracks during the macroscopic survey. Thus, isolated swarm tracks most likely account for the high-track density of Tray 2. In general, it appears as if Tray 1 and Tray 2 intercepted grossly identical populations of particles, except for the human waste-products which dominate Tray 1, consistent with the location of Shuttle and associated practices of waste-dumping.